International Journal of Advances in Engineering and Management (IJAEM)
Volume 6, Issue 07 July 2024, pp: 393-401 www.ijaem.net ISSN: 2395-5252

Spatiotemporal Analysis of Land Use and Land Cover Types and Their Impacts on Land Surface Temperature of Anambra State, Nigeria

Ukanwa, S. O., Ejikeme, J. O and Eze, F.C.

Department of Surveying and Geoinformatics, Nnamdi Azikiwe University, Awka, Anambra State

Date of Submission: 10-07-2024 Date of Acceptance: 20-07-2024

ABSTRACT

The uncontrolled rapid urban expansion and landuse/ landcover transformations alters the hydrological, thermodynamic, and radioactive activities of the earth surface, and this amplifies the effects of climate change and heat waves. This study was aimed at performing a spatiotemporal analysis of land surface temperature and its impact on land use/land cover types in Anambra State of Nigeria. Lansat 8 OLI imageries of 2013, 2018 and 2023 were used for data analysis to retrieve the land surface temperature (LST) and the land use/ land cover (LULC) types. The methodology adopted by study for LST retrieval was the Single Channel Algorithm (SCA) and for classifying the LULC, the Supervised Classification using Maximum Likelihood Classifier (MLC) algorithm was used. The ArcGIS 10.8 was used to classify LULC types and estimate the LST. The findings suggest that because of the biophysical properties of the land surfaces, LULC has a considerable impact on LST values.. The greatest LST variations were found between water bodies and vegetation, but moderate LST differences were found between bare lands and vegetation as well as between barren land and built-up regions. The study also revealed that the state's major cities, like Onitsha, Awka and Nnewi, usually have the highest LSTs. The study will have a positive health impact in the study area and help policies makers and relevant agencies in making an information decision and policies based on the findings from the study.

KEYWORDS: Land Use/Land Cover (LULC) classification, LST, SCA and SCA

I. INTRODUCTION

In urban areas, landuse/ landcover changes are a critical factor affecting the physical characteristics of the Earth's surface due to the unique characteristics that each landuse and landcover (LULC) category possesses with respect to radiation and absorption of energy on the Earth's surface (Koko et al., 2021).These changes affect the degree of absorption of solar radiation, albedo, surface temperature, evaporation rates, transmission of heat to the soil, storage of heat, wind turbulence, can drastically alter the conditions of the near-surface atmosphere over the cities (Mallick et al., 2008), modify energy and water balance processes as well as playing a vital role in many environmental processes (Weng et al., 2004). The land surface temperature can be considered an effective measure for predicting radiation budgets for heat balance, it can be an important indicator in understanding the interactions that occur between the environment and humans in urban environments and also an important factor controlling the physical and biological processes of land systems (Tan et al., 2010). Furthermore, the increase in land surface temperature effects the urban heat island (UHI) phenomena, having a significant influence on biodiversity's primary function, local and regional climate (Luck and Wu, 2002).

As a result of the spatiotemporal landuse/ landcover variations, this alters on the pattern of a variety of land surfaces of spatial landscapes and it is therefore critical to ascertain landuse/ landcover changes at appropriate scales using accurate time series data. Studies have shown that land cover changes influence the surface temperature due to the different heat capacity of soils associated to a given amount of solar radiation (Fonseka et al., 2019).

Anambra State, located in southeastern Nigeria, has experienced considerable LULC changes over the past few decades. This study aims to analyze the spatiotemporal dynamics of these changes and assess their impacts on land surface temperature (LST), a critical parameter influencing local climate and environmental conditions.

II. MATERIALS AND METHODS

2.1 Study Area

Anambra State is located in the southeastern region of Nigeria and is one of the 36 states in the country. It lies between latitudes 5.7°N and 6.8°N and longitudes 6.4°E and 7.4°E. The state covers an area of about 4,844 square kilometers and it is bounded by Delta State to the west, Imo State and Rivers State to the south, Enugu State to the east, and Kogi State to the north. It is characterized by diverse geographical features, including the Anambra River, which is a tributary of the Niger River, and various uplands and valleys.The climate of the Anambra State is tropical rainforest climate, characterized by two main seasons: the rainy season (April to October) and the dry season (November to March). The average annual temperature is around 27°C (81°F). As of the 2006 census, Anambra State had a population of approximately 4.18 million people. The population is predominantly Igbo, one of the largest ethnic groups in Nigeria. The state has a high population density, reflecting its relatively small geographic size compared to its large population.
Fig. 1 shows the map of the study area.

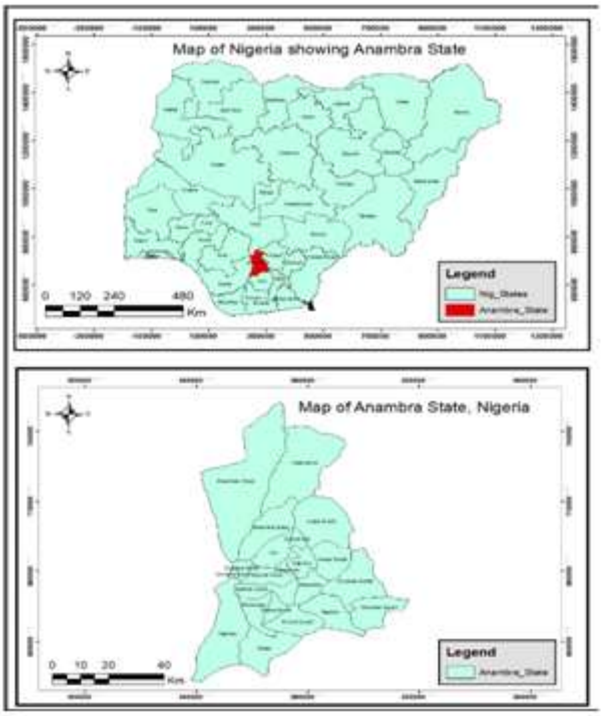

Fig 1: Map of the study area

2.2 Materials

In this study, Table 1. shows the different datasets used for this study and their sources.

S/N	Data	Acquisition Date	Scale	Source
1	Landsat 8 OLI_TIRS	2013-07-23	30m TM	U.S. Geological Survey(USGS)
2	Landsat 8 OLI_TIRS	2018-06-10	30m TM	U.S. Geological Survey(USGS)
3	Landsat 8 OLI_TIRS Google	2023-07-18	30m TM	U.S. Geological Survey (USGS)
4	Earth Data			Google Earth
5	Administrative Map ofAnambra State			OSGOF

International Journal of Advances in Engineering and Management (IJAEM)
Volume 6, Issue 07 July 2024, pp: 393-401 www.ijaem.net ISSN: 2395-5252

2.3 Methods

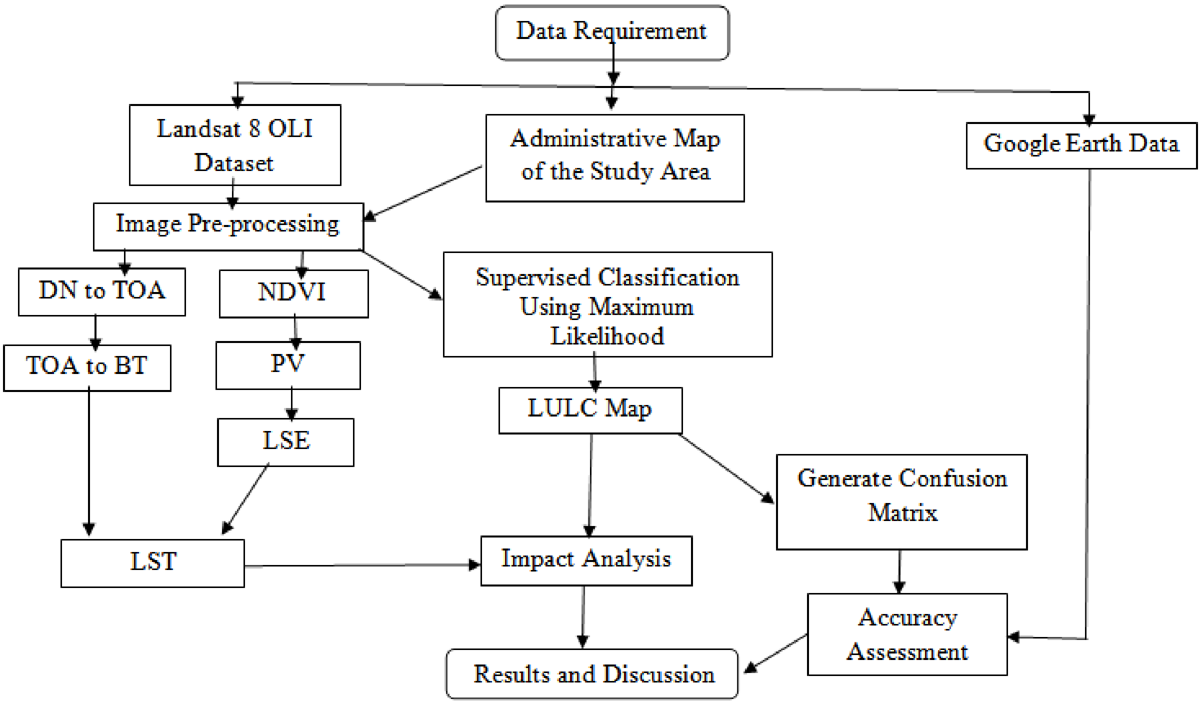

Fig 2: Flowchart of methodology adopted by the study

Source: The Author

2.4 Image Processing and Classification

The supervised classification approach was used to the Landsat 8 OLI imageries for LULC categorization. The training samples for the supervised classification operation were made using the previous information of the research region. Using polygons drawn in an area of interest (AoI) layer in the satellite images, training samples were produced. The supervised classification classifier was the maximum likelihood algorithm, and the signature file was generated. Over the years, medium-resolution satellite data, such as that obtained from Landsat 8 OLI, has been classified extensively using the maximum likelihood classifier (MLC).The maximum likelihood classifier uses a statistical method to identify patterns, and it makes the assumption that each class's statistics in each image band have a normal distribution. The algorithm's implementation is straightforward and extensively utilized for diverse remote sensing applications. It calculates the likelihood that a particular pixel belongs to each class and designates it accordingly (Ahmad and Quegan, 2012).

Table 2.0 shows the different land use and land cover types for the study.

Table 2: Description of land cover types for the study.

S/N	LULC Category	Description
1.	Built-up lands	All residential, commercial, and industrial areas, village settlements, and transportation infrastructure
2	Vegetation covers	Trees, shrub land and semi-mature vegetation, deciduous, coniferous, and mixed forests, palms, orchids, herbs, gardens, and grasslands
3	Bare land	Naturally occurring soils with no vegetation cover or above-ground cover within the study area.
4	Water bodies	River, permanent open water, lakes, ponds, canals, and Reservoirs

International Journal of Advances in Engineering and Management (IJAEM)
Volume 6, Issue 07 July 2024, pp: 393-401 www.ijaem.net ISSN: 2395-5252

2.5Accuracy Assessment

This study used the confusion/error matrix to perform an accuracy evaluation in order to ascertain the correctness and reliability of the land use and land cover data. As noted by Hasmadi et al. (2009), evaluating the accuracy of image classification is a crucial phase in ascertaining the dependability of the outcomes acquired from the classification procedure. Anderson (1997) said that when identifying land cover classes from remotely sensed data, at least 85% interpretation accuracy should be achieved.To calculate for the producer accuracy, user accuracy, and overall accuracy Equation (1) was used.

$$\text{Overall Accuracy (\%)} = \frac{\text{Total Number of correctly classified samples}}{\text{Total number of samples}} \times 100 \quad \text{......(1)}$$

$$\text{Kappa} = \frac{P(a) - P(e)}{1 - P(e)} \quad \text{......(2)}$$

Where,
P(a) is the relative observed agreement
P(e) is the hypothetical probability of chance agreement.

2.6 Land Surface Temperature Retrieval

Using the Single Channel Algorithm (SCA) to get land surface temperature (LST) from thermal bands of a satellite image is a complex undertaking that requires a number of steps. The Landsat 8 OLI imageries were utilized for this purpose.

2.6.1 Conversion of Digital Numbers to Top-of-Atmosphere (TOA)

The conversion of spectral radiance digital numbers (DNs), which are contained in the thermal data of the Landsat sensor, into radiance units is the first step in calculating the Landsat surface temperature (LST). This method gives a way to represent pixels that haven't been calibrated yet.
The following equation is used:

$$L\lambda = ML \times Q_{cal} + AL - O_i \quad \text{.................................. .... (3)}$$

Where,
$L\lambda$ is the TOA spectral radiance in Watts/ (m^2.sr. µm)
ML is the band-specific multiplying rescale factor in the metadata
AL is the band-specific additive rescaling factor in the metadata
Q_{cal} is the calibrated and quantized pixel values (DN),
O_i represents the offsets supplied by USGS for the TIRS band calibration (Sobrino et al., 2004).

2.6.2 Conversion of Radiance to Brightness Temperature (BT)

It is necessary to convert the converted TOA to brightness temperature (BT) by eliminating the atmospheric impacts in the thermal zone (Barsi et al., 2005). This is computed using pre-launch calibration constants and the assumption of unity emissivity. In order to update the radiant temperature, add absolute zero (around −273.15 ◦C). To achieve this, the following equation and the thermal constants listed in the metadata file were used.

$$BT = \frac{K2}{Ln(K1/L\lambda + 1)} - 273.15 \quad \text{......(4)}$$

Where,
Lλ is the TOA spectral radiance
K1 is the Band 10 constant band-specific thermal conversions from the metadata
K2 is the Band 11 constant band-specific thermal conversions from the metadata.

2.6.3 Calculating of Normalized Difference Vegetative Index (NDVI)

Due to its dependence on variables like land surface emissivity and proportional vegetative index (PV), the NDVI is a crucial component in the computation of land surface temperature (LST). The NDVI was computed using the following equation:

$$NDVI = \frac{NIR - Red}{NIR + Red} \quad \text{......(5)}$$

Where,
NIR is near-infrared band
Red is red band.
For this study, Landsat 8 OLI data was utilized and the near infrared is Band 5 while Red is Band 4.

2.6.4 Calculating Proportionate Vegetation Index (PV)

According to Sobrino et al., (2004), the PV is the vegetation proportion viewed by derived using the following equation:

International Journal of Advances in Engineering and Management (IJAEM)
Volume 6, Issue 07 July 2024, pp: 393-401 www.ijaem.net ISSN: 2395-5252

$$PV = \frac{NDV - NDVI\,min}{NDVI\,max - NDVI\,min} \quad \text{.................................(6)}$$

Where,
NDVI max is for vegetation and NDVI min is for bare ground

2.6.5 Calculating Land Surface Emissivity (LSE)

An essential component in determining the LST is the land surface emissivity (Darren et al., 2020). This proportionality factor represents the efficiency of transmitting thermal energy across the surface into the atmosphere and scales blackbody radiance (Planck's law) to predict emitted radiance. The LSE can be calculated using the following equation

$$LSE = \varepsilon S \times (1 - Pv) + (\varepsilon V \times Pv) \quad \text{...(7)}$$

Where,
εV and εS are the vegetation and soil emissivity, respectively
Pv is the proportionate vegetation index
For this study, the emissivity constants of Band 10 of Landsat 8 OLI was used which are $\varepsilon S = 0.971$ and $\varepsilon V = 0.987$ respectively.

2.6.6 Calculating Land Surface Temperature (LST)

$$LST = \frac{BT}{1 + \left(\frac{BT}{\rho}\right) Ln\,LSE} \quad \text{...(8)}$$

Where,
BT is at-sensor brightness temperature,
$\rho = h \times c/\sigma = 1.438 \times 10^{-2}$ mK, and it is further converted to μm units
Furthermore, h is Planck's constant (6.626 × 10-34 Js), σ is the Boltzmann constant (1.38×10^{-23} J/K) and c is the velocity of light (2.998 × 108 m/s) (Avdan and Jovanovska, 2016).

2.7LULC Types Impacts Analysis on LST

To ascertain the effects of LULC types on LST of Anambra State, the data of LULC and LST were combined. This was accomplished using the data integration method in ArcGIS.

III. RESULTS AND DISCUSSION

3.1 Classification Results

The results of the LULC Analysis using supervised classification method from 2013 to 2023 are presented in Fig 3 and Table 3 respectively.

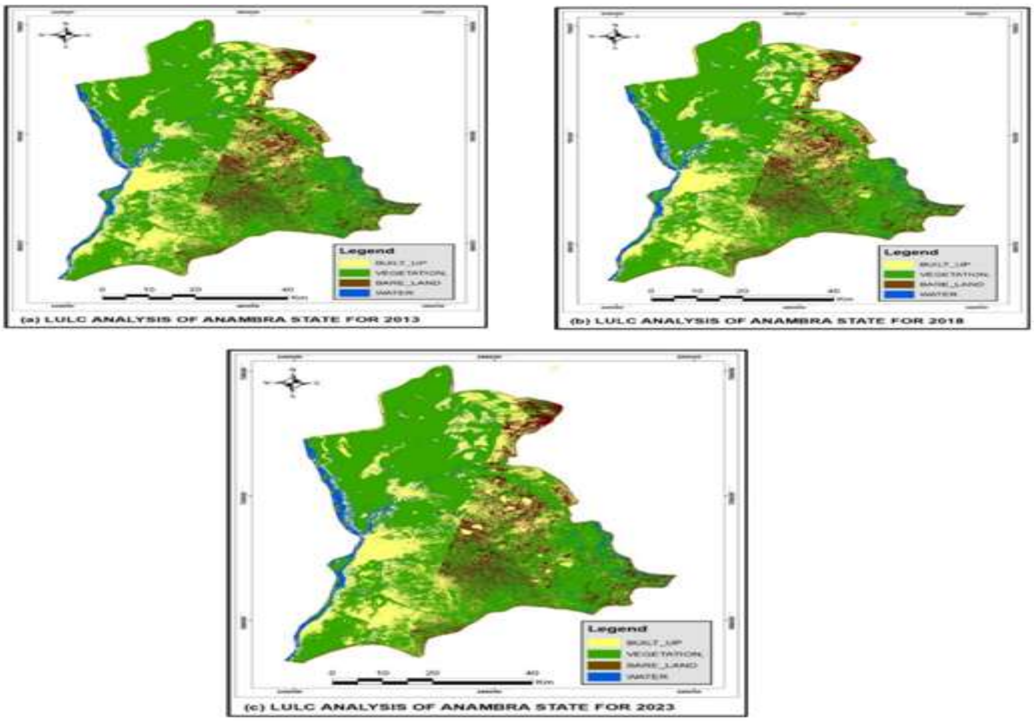

Figure 3: Classified Maps of (a) 2013, (b) 2018, and (c) 2023

Table 4: Classification Results

Year	Built-up Areas (Sq.Km)	Vegetation (Sq.Km)	Bare Lands (Sq.Km)	Water Bodies (Sq.Km)
2013	921.371 (18.94%)	3634.891 (74.72%)	142.049 (2.92%)	166.372 (3.42%)
2018	1006.016 (20.68%)	3557.543 (74.13%)	147.886 (2.04%)	153.238 (3.15%)
2023	1135.903 (23.35%)	3406.738 (71.03%)	177.074 (2.68%)	143.022 (2.94%)

The results as shown in Fig 3 and Table 3, in 2013, vegetation occupied the highest landuse area 3634.891Sq. Km(74.72%), followed by built-up areas with 921.371 Sq. Km (18.94%), bare lands with 142.049 (2.92%) and water bodies with 166.372 (3.42%). In 2018, vegetation occupied the highest area with 3557.543 (74.13%), followed by built-up areaswith 1006.016 (20.68%),the bare lands and water bodies occupies 147.886 (2.04%)and 153.238 (3.15%) respectively. In 2023, vegetation occupied the highest area 3406.738 (71.03%), followed by built-up areas 1135.903 (23.35%), the bare lands and water bodies occupies 177.074 (2.68%) and 143.022 (2.94%) respectively.

3.2 Classification Accuracy Assessment

The accuracy and dependability of the study's land use and land cover analysis were assessed using the confusion/error matrix. Tables 4, 5, and 6 shows the accuracy assessment findings, accordingly.

Table 4: Classification Accuracy Assessment for 2013

Landuse Classes	Built- up	Vegetation	Bare Lands	Water bodies	Total	User's Acc. (%)
Built- up	64	0	2	0	66	96.97
Vegetation	0	45	0	2	47	95.74
Bare Lands	2	0	57	0	59	96.61
Water bodies	0	3	0	57	60	95.00
Total	66	48	59	59	232	
Producer's Acc. (%)	96.97	93.75	96.61	96.61		
Overall Acc. (%)	96.12					
Kappa Coefficient	0.96					

Table 5: Classification Accuracy Assessment for 2018

Landuse Classes	Built- up	Vegetation	Bare Lands	Water bodies	Total	User's Acc. (%)
Built- up	64	0	1	0	65	98.46
Vegetation	0	48	0	1	49	97.96
Bare Lands	3	0	57	0	60	95.00
Water bodies	0	3	0	57	60	95.00
Total	67	51	58	58	234	
Producer's Acc. (%)	95.52	94.12	98.28	98.28		
Overall Acc. (%)	96.58					
Kappa Coefficient	0.97					

International Journal of Advances in Engineering and Management (IJAEM)
Volume 6, Issue 07 July 2024, pp: 393-401 www.ijaem.net ISSN: 2395-5252

Table 6: Classification Accuracy Assessment for 2023

Landuse Classes	Built- up	Vegetation	Bare Lands	Water bodies	Total	User's Acc. (%)
Built- up	66	0	1	0	67	98.51
Vegetation	0	52	0	2	54	96.30
Bare Lands	2	0	53	0	55	96.36
Water bodies	0	3	0	53	56	94.64
Total	68	55	54	55	232	
Producer's Acc. (%)	97.06	94.55	98.15	96.36		
Overall Acc. (%)	96.55					
Kappa Coefficient	0.97					

3.3 Land Surface Temperature (LST) Results

The Single Channel Algorithm (SCA) was used to get the LST. Utilizing the study's Landsat 8 OLI imagery, the LST were successfully extracted using the Raster Calculator Tools in the ArcGIS software suite. Fig. 4 presents the findings.

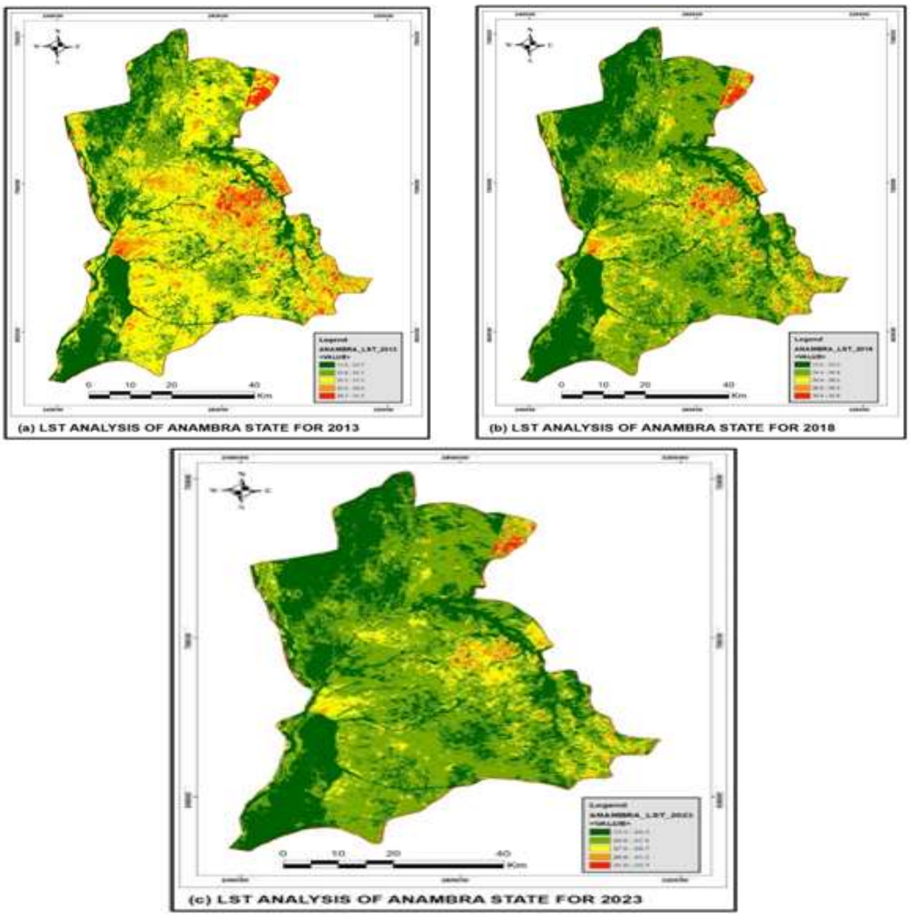

Figure 4: LST Maps of (a) 2013, (b) 2018, and (c) 2023

International Journal of Advances in Engineering and Management (IJAEM)
Volume 6, Issue 07 July 2024, pp: 393-401 www.ijaem.net ISSN: 2395-5252

The results as shown in Fig 4, in 2013 it was observed that the LST range is from 13.5◦C to 31.7◦C. The lowest LST was 13.5◦C while the highest LST was 31.7◦C while in 2018, the LST range is from 13.5◦C to 32.8◦C. The lowest LST was 13.5◦C while the highest LST was 32.8◦C. and in 2024, the LST range is from 13.5◦C to 33.7◦C. The lowest LST was 13.5◦C while the highest LST was 33.7◦C.

3.4 Impact of LULC Types on LST Results

The different LULC types were analyzed to determine their various impacts on LST. The results of the analysis were presented in Table 7.

Table 7: Impact of LULC Types on LST of Anambra State from 2013 to 2023

Year	Built-up LST	Vegetation LST	Bare Land LST	Water LST
2013	18.94% 25.2◦C-31.7◦C	74.72% 23.7◦C-27.5◦C	2.92% 25.2◦C-27.5◦C	3.42% 13.5◦C-23.7◦C
2018	20.68% 26.9◦C-32.8◦C	74.13% 24.4◦C-26.8◦C	2.04% 24.4◦C-26.8◦C	3.15% 13.5◦C-24.3◦C
2023	23.35% 27.6◦C-33.7◦C	71.03% 24.5◦C-27.5◦C	2.68% 24.6◦C-27.5◦C	2.94% 13.5◦C-24.5◦C

From the results in Table 7, in 2013, it was observed thatbuilt-up areas had the highest LST range, with an average LST range of 25.2◦C to 31.7◦C. Bare lands had the second highest LST range, at 25.2◦C to 27.5◦C. Vegetation had the third highest LST range, at 23.7◦C to 27.5◦C, and water had the lowest, at 13.5◦C to 23.7◦C. In addition, it was noted that, for 2018, the highest LST range was found in built-up areas, where it averaged 26.9◦C–32.8◦C; the second highest LST range was found in bare lands, where it was 24.4◦C–26.8◦C; the third highest LST range was found in vegetation, where it was 24.4◦C–26.8◦C; and the lowest waswater with an LST range of 13.5◦C-24.3◦C.Furthermore, it was noted in 2023 that the highest LST ranges were found in built-up areas, with average LST ranges of 27.6◦C-33.7◦C; bare lands had the second-highest LST ranges, at 24.6◦C-27.5◦C; vegetation had the third-highest LST ranges, at 24.5◦C-27.5◦C; and water had the lowest, at 13.5◦C-24.5◦C.

IV. CONCLUSION

This study investigated into how different Land Use and Land Cover (LULC) types affected Land Surface Temperature (LST) in Anambra State. The results suggest that because of the biophysical properties of the land surfaces, LULC has a considerable impact on LST values. It is suggested that incorporating vegetation into urban areas on a regular basis can assist maintain a cooler urban thermal environment since both vegetation and water bodies reduce surface temperatures. The greatest LST variations were found between water bodies and vegetation, but moderate LST differences were found between bare lands and vegetation as well as between barren land and built-up regions. The study also revealed that the state's major cities, like Onitsha, Awka and Nnewi, usually have the highest LSTs.

The studyrecommend the following:
i. To guarantee sustainable growth in Anambra State, more study and observation should be carried out.
ii. In order to lower the high LST in built-up and urban areas, it should be encouraged to establish green spaces and greeneries.
iii. A sustainable state development strategy to manage agricultural and grazing operations, among other anthropogenic activities.

REFERENCES

[1]. Anderson, J.R.(1997). Land use classification schemes used in selected recent geographic applications of remote sensing, Photogrammetric Engineering, 37 (4) 379–387.
[2]. Avdan, U., and Jovanovska, G. (2016). Algorithm for Automated Mapping of Land Surface Temperature Using LANDSAT 8 Satellite Data. Journal of Sensors.
[3]. Barsi, J. A., Schott, J. R., Palluconi, F. D., and Hook, S. J. (2005). Validation of a web-based Atmospheric correction tool for single thermal band instruments (Conference session). Proceedings SPIE, 58820 E, Bellingham, WA, p. 7.
[4]. Darren, H. J. A., Mohd, H. I. and Farrah, M. M. (2020).Land Use/Land Cover Changes and the Relationship with Land Surface Temperature Using Landsat and

International Journal of Advances in Engineering and Management (IJAEM)
Volume 6, Issue 07 July 2024, pp: 393-401 www.ijaem.net ISSN: 2395-5252

MODIS Imageries in Cameron Highlands, Malaysia. Land 2020

[5]. Fonseka, H.P.U., Zhang, H., Sun, Y., Su, H., Lin, H., and Lin, Y. (2019). Urbanization and its impacts on land surface temperature in Colombo metropolitan area, Sri Lanka, from 1988 to 2016. Remote Sensing, 11 (8, 957), 18 pp

[6]. Hasmadi, M., Pakhriazad, H.Z. and Shahrin, M.F. (2009). Evaluating supervised and unsupervised techniques for land cover mapping using remote sensing data, Malaysian Journal of Social Space, 5 (1) 1–10

[7]. Hossain, M.S., Arshad, M., Qian, L., Kächele, H., Khan, I., Islam, M.D.I, Mahboob, M.G., 2020. Climate change impacts on farmland value in Bangladesh. Ecological Indication. 112,106181.

[8]. Luck, M., Wu, J., 2002. A gradient analysis of urban landscape pattern: a case study from the Phoenix metropolitan region, Arizona, USA. Landscape Ecology, 17, 327–339.

[9]. Mallick, J., Kant, Y., & Bharat, B. (2008). Estimation of land surface temperature over Delhi using Landsat-7 ETM+. Journal of Indian Geophysical Union, 131-140.

[10]. Sobrino, J.A., Munoz, J.C.J. and Leonardo, P. (2004). Land surface temperature retrieval from LANDSAT TM 5. Remote Sensing of Environment, 434 – 440

[11]. Tan, K.C., San Lim, H., MatJafri, M.Z. and Abdullah, K. (2010). Landsat data to evaluate urban expansion and determine land use/land cover changes in Penang Island, Malaysia. Environmental Earth Science. 60, 1509–1521.

[12]. Weng, Q. (2001). A remote sensing-GIS evaluation of urban expansion and its impact on surface temperature in the Zhujiang Delta, China. International Journal of Remote Sensing, 22.